University of Reading

School of Mathematical and Physical Sciences

Department of Mathematics and Statistics

Rain drop growth by collision and coalescence

Peter Barnet

August 2011

Abstract

The numerical scheme proposed by Bott to simulate the growth of cloud droplets is used to investigate the aspects to which the collision and coalescence growth mechanism is sensitive. Perturbations to the initial size and concentration of the cloud droplets are considered, as well as modi cations to the shape of the initial droplet distribution. The impact of these changes

Chapter 1

Introduction

A fundamental problem with existing models that simulate the growth of

a new drop of mass equal to the sum of the two original droplet masses, then we say the drops have coalesced. The following schematic highlights a situation when collision and coalescence may occur.

Figure 1.1: schematic of how two drops can collide

In this schematic (gure 1.1) a drop of mass m_2 falling at terminal velocity v_2 is on course to collide with a smaller drop of mass m_1 falling at its terminal velocity v_1, since $v_2 > v_1$. If the two drops combine (coalesce) when they collide then we obtain the situation shown in gure 1.2.

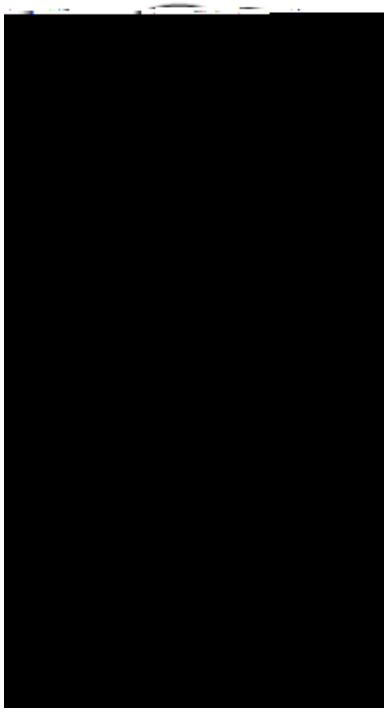

Figure 1.2: schematic of coalesced drops

The new drop that forms has mass that is simply the sum of the two colliding droplet masses, and terminal velocity equal to the sum of the velocities of the colliding drops. The larger of the two colliding drops is referred to as the collector drop and is considered to be drop that gains the mass at the expense of the smaller drop in the collision. This smaller drop is usually called the collected drop.

The collision and coalescence of cloud droplets is quite a complicated process, and one reason for this is the fact that an initial droplet size spectrum must

collector drops this small (associated with the drops following the air ow around eachother and avoiding collision).

When two droplets collide it can result in the break up of the collector drop, or simply the two drops moving apart fairly unchanged. Davis and Sartor

SCE in terms of the change in the drop number distribution function with time, we can write it in terms of the change in the mass distribution function $g(y;t)$, where

$$g(y;t)dy = xn(x;t)dx; \quad n(x;t) = \frac{1}{3x^2}g(y;t): \tag{1.2}$$

Here $y = \ln r$ with r being the radius of the drops with mass x. The mass distribution function basically describes how the total water mass is distributed in drops of di erent sizes. If we substitute (1.2) into (1.1) we obtain the SCE describing the change in the mass distribution function with time,

$$\frac{@g(y;t)}{@t} = \int_{y_0}^{y_1} \frac{x^2}{x_c^2 x'} g(y_c;t)K(y_c;y')g(y';t)dy' \int_{y_0}^{1} g(y;t)\frac{K(y;y')}{x'}g(y';t)dy' \tag{1.3}$$

where $y_c = \ln r_c$ and $y' = \ln r'$ with r_c and r' being the radius of drops of mass x_c and x' respectively. The rst integral on the right hand side of (1.3) represents the rate at which drops of mass x are gained by collision and coalescence of two smaller drops. The second integral describes the loss of drops of mass x due to collection by other drops.

In this paper we will explore the aspects to which the collision and coalescence growth mechanism is sensitive, with the aim of trying to explain how the rapid formation of rain seen in convective clouds is possible. To do

the scheme Bott used are given in the following section.

1.1 Numerical methods for solving the SCE

A popular numerical method to approximate the SCE was devised by Berry and Reindhart (1974). They solved (1.1) at discrete points of the drop spectrum giving very accurate results. However the problem with the scheme they used was that due to the number of calculations that must be made, the method was not very computationally e cient and so it was slow to yield results.

A new ux (nite volume) method was proposed in 1998 by Bott. The instant advantage of this method over the scheme devised by Berry and Reindhart is that it is very computationally e cient. The method Bott devised is now brie y described, but greater detail can be found in Bott (1998).

To solve (1.3) numerically a logarithmically equidistans ridm n

, teoonese to the in ridm b,
uc(ed,)]TJ/215 11.9552 Tf 26.0669 -43.338 Td [x
Frcome yield
ltt hopudt be(nosed)-564(that)]TJ/215 11.9552 Tf1403776 03 Td [mE
,
apodntd,

grid boxes. y_k = ln =3 from the fact that y = ln r and x / r^3 (which we know from the relation *Mass* = *Density* *Volume*, where *Volume* = $\frac{4}{3}$ r^3). Since can be thought of as a change in mass, we can write y / ln $\frac{1}{3}$. It therefore follows that because we are considering the grid spacing (change in y over a grid box), we can write y_k = ln $\frac{1}{3}$ which is just expressed more simply as y_k = ln =3.

The collision of drops with mass x_i with drops of mass x_j yields a change in the mass distributions g_i,g_j. In discretized form the change in the mass distributions may be expressed as,

$$g_i(i;j) = g_i \quad g_i \frac{K(i;j)}{x_j} g_j \quad y \quad t \tag{1.5}$$

$$g_j(j;i) = g_j \quad g_j \frac{K(j;i)}{x_i} g_i \quad y \quad t \tag{1.6}$$

In these discretizations, g_i and g_j represent the mass distribution functions at grid point i and j resp11.955270-254(g)-255(p)-27(oin)27(t)]T8s1.9552 T/eb8(8rid)-25511.955 j $54(g)$-255(p)-27(oin)27(t)]T8s1.9552 T/eb8(8rid)-25511.955

Collisions between drops in grid box *i* with drops in grid box

shown in the following schematic by Bott.

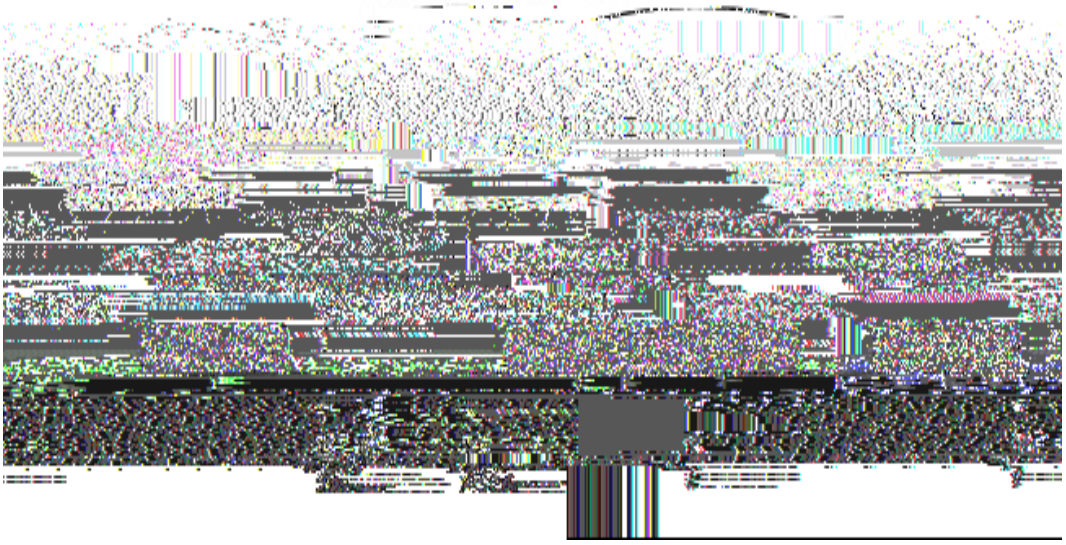

Figure 1.3: Schematic illustration of the ux method (Bott 1988)

In gure 1.3, the dashed lines represent the initial mass distributions in grid boxes $i; j; k;$ and $k + 1$, and the full lines indicate the mass distributions after the collision process. The stippled area in grid box k corresponds to the mass that will be transported into grid box $k + 1$, and the dark shaded areas are the nal mass increase in grid boxes k and $k + 1$.

This mass advection may be written as,

$$g_k(i; j) = g_k^0(i; j) \quad f_{k+1=2}(i; j) \tag{1.10}$$

$$g_{k+1}(i; j) = g_{k+1} + f_{k+1=2}(i; j); \tag{1.11}$$

where

$$\frac{f_{k+1=2}(i;j) \quad y}{t}$$

represents the mass ux through the boundary $k + \frac{1}{2}$. To obtain the results in this paper we will calculate $f_{k+1=2}(i;j)$ using the upstream formula Bott proposed, although it should be noted he tried two additional approaches to determine the ux. The upstream formula gives,

$$f_{k+1=2}(i;j) = c_k g_k^0(i;j) w(i;j): \tag{1.12}$$

In this formula we should interpret c_k as a Courant number, and should calculate it as a function of the position $x^0(i;j)$ between x_k and x_{k+1} as below.

$$c_k = \frac{x^0(i;j) \quad x_k}{x_{k+1} \quad x_k} \tag{1.13}$$

A weighting function $w(i;j)$ has been introduced in (1.12) because the advective ux through the boundary $k + \frac{1}{2}$ is given by $g^0(i;j)$ instead of $g_k^0(i;j)$, unlike for the normal advection process with $c_k = 1$ (for $x^0(i;j) = x_{k+1}$). As a result,

$$w(i;j) = \frac{g^0(i;j)}{g_k^0(i;j)}; \tag{1.14}$$

and hence it is clear that the upstream scheme is simply,

$$f_{k+1=2}(i;j) = c_k g^0(i;j): \tag{1.15}$$

This results in the same partitioning of $g^0(i;j)$ as that in the method of Kovetz and Olund (1969), except they solved the SCE in terms of number distribution, as in (1.1). Bott found that this upstream formula produces drop spectra that are seemingly too broad, and he knew this to be due to the large numerical di usion that results from such an advection scheme. The two other approaches he tried determined the ux according to higher order advection schemes of Bott (1989a,b), and through using these the numerical di usion was reduced.

An iterative procedure is needed in order to treat all the collisions of drops during the time step t. If the grid box of the smallest and largest drops being involved in the collision process are denoted by $i = i_0$ and $i = i_1$, then rstly collision of the smallest drops with drops of grid box $j = i_0 + 1$ is calculated giving new mass distribution functions according to equations (1.5),(1.6),(1.10) and (1.11). Next the collision of the drops remaining in $i = i_0$ having the new mass distribution function $g_{i_0}(i_0; i_0 + 1)$ with the drops in grid box $j = i_0 + 2$ is determined. This process is continued until all the collisions of drops in grid box $i = i_0$ with drops of grid boxes $j = i_0 + 1; i_0 + 2; :::; i_1$ have been considered. Next collisions of drops in grid box $i = i_0 + 1$ with all larger drops $j = i_0 + 2; i_0 + 3; :::; i_1$ are treated in the same way, and this is repeated for all drops $i = i_0 + 2; :::;$ until in the last

step the collision of drops $i = i_1 \quad 1$ with drops $j = i_1$ has been determined.

It is clear from equations (1.5) and (1.6) that $g_i(i;j)$ or $g_j(j;i)$ could become negative which is obviously a problem because negative mass concentrations are unphysical. It is therefore required that the ux method is positive definite, and this can be insured by applying the following restrictions to the numerical time step:

$$t \quad \frac{x_j}{g_j(i;j \quad 1) \quad yK(i;j)} \tag{1.16}$$

$$t \quad \frac{x_i}{g_i(i;j \quad 1) \quad yK(i;j)} \tag{1.17}$$

where inequality (1.17) is valid for $j \neq k$. The rst inequality (1.16) ensures that $g_i(i;j) \quad 0$ after each collision. The reason why (1.17) does not apply if $j = k$ is that for $j = k$ the mass subtracted from $g_j(j;i)$ in (1.6) will be added again in (1.9).

Earlier in this section the collection kernel $K(i;j)$ was mentioned, and this quantity is related to the probability that in a given time interval there will be a collection event involving two droplets. In Bott's model three di erent calculation methods are considered for the kernel, these including the Golovin kernel (taken from Golovin 1963), and the hydrodynamic kernels. The Golovin kernel will not be described or used at any point to obtain results in this paper, however results are presented for the other two kernels,

and so these are now brie y described.

The hydrodynamic kernel is given (from Pruppacher and Klett 1997) by the following:

$$k(i;j) = (r_i + r_j)^2 E\, jw(r_i) \quad w(r_j)j \tag{1.18}$$

In (1.18) r_i and r_j represent the radii of the two colliding drops respectively, and $w(r_i)$, $w(r_j)$ correspond to the terminal velocities of the two drops, obtained following Beard (1976). E is the collision e ciency and in this report

collector drops of radius < 30 *m* Hall chose the theoretical results of Davis (1972) and Jonas (1972). For collecting droplets of radii between 40 and 300 *m*, which are collecting smaller drops with radius < 60% the size of the collector drop radius the results of Schlamp *et al.* (1976), Lin and Lee (1975)

Chapter 2

Methodology

From the previous work on this field it appears that the growth process is sensitive to both the size and the initial concentration of droplets within the cloud. In order to quantify the growth rate of these model simulated drops, we introduce a function that calculates the time taken to produce rain drops in the cloud. Since raindrops can be a large range of sizes, a fixed radius value had to be chosen in the model, so as to be consistent for comparisons. This radius was chosen to be 1mm, which is a typical radius for a raindrop in a convective cloud. The model from Bott (1998) was adapted so as to indicate that rain was being produced when more than 50 percent of the total water in the cloud was in drops of radius greater than 1mm, this way avoiding the issue that chance collisions might produce a few drops of this size very quickly, which would lead to the model suggesting a growth rate that may be unrealistically fast.

As stated earlier, in Bott's simulations the initial mode radius of the cloud

drops was chosen to be 10

tion from the collision e ciency di ers for the di erent calculation methods (as the contribution from $(r_i + r_j)^2$ and $w(r_i)$ $w(r_j)$ will be the same in each case). This breaking up of the kernel will also allow us to observe the relative importance of the three componence under di erent collision scenarios (di erent sizes of droplets colliding).

Chapter 3

Results

We first examine the growth rate of the cloud droplets for the initial distribution considered by Bott, with an initial mode radius of 10 m and a total water content of 1 gm^{-3}, just to see if we can replicate the results he obtained.

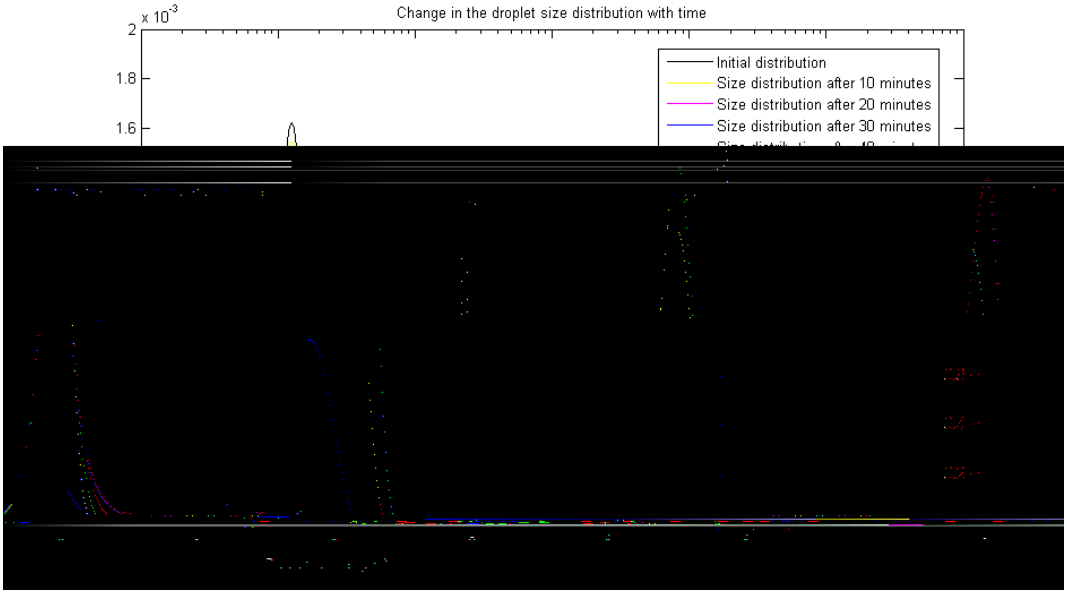

Figure 3.1: Droplet size evolution for an initial mode radius of 10 *m* and a total water content of 1 gm^{3}

From gure 3.1 we can observe that the average size of the droplets clearly increases with time as over the course of an hour the mean radius has become larger by about two orders of magnitude. For the rst 30 minutes there does not appear to be a great amount of change in the distribution, with much of the mass still centred in a peak close to 10 m. The amount of mass in this peak can however be seen to be slowly decreasing in this period, and after 30 minutes there is clear evidence of larger drops having been formed as quite a broad hump, centred close to 200 m has appeared. The mass in the initial peak is decreasing because drops are colliding and coalescing forming larger drops. If we refer to equation (1.3) we can explain this loss of mass in the initial peak by the rst integral, as this represents the increase in the number

of larger drops due to collisions between the smaller (initial) drops.

The most substantial change in the distribution occurs in the 10 minute interval following the distribution described after 30 minutes, as after 40 minutes most of the mass is in a peak centred close to 1 mm (1000 m), which is quite a shift from the situation seen 10 minutes earlier where most of the mass was still in drops of radius close to 10 m. An explanation for this sudden shift comes from the fact that we would expect the larger drops that have clearly formed after 30 minutes to rapidly collect the smaller drops. This is thought because if we refer to equation (1.18) it is obvious that the collection kernel will be larger for these type of collisions (compared to that for collisions between the smaller initial drops with other small drops). This is due to the $(r_i + r_j)^2$ component being larger, and also the di erence in terminal velocity component $(w(r_i) \quad w(r_j))$ being larger552th-271(drops)d5s.o15 11.552 6lscem6

dictated by the collision kernel, which is dependent on the size of the colliding droplets (the kernel value increases with colliding droplet size). We will further investigate this sensitivity to the collision kernel later in the report.

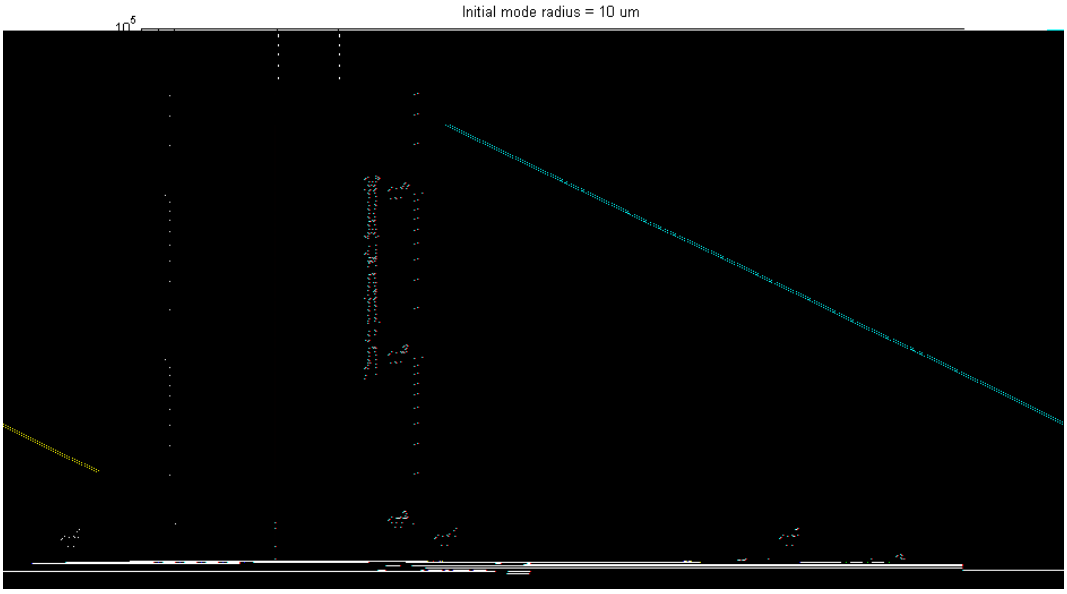

Figure 3.2: Time taken to produce rain for varying total water contents but with the initial mode radius of droplets xed to 10 *m*

We next explore the time taken for the model to produce rain (50% of the mass in drops of radius greater than 1mm), through perturbing the total water content from the default 1 gm^{3} (gure 3.2). The initial mode radius has not been changed here, so simply increasing the water content gives more drops, and likewise reducing it gives fewer drops. As we might expect, it would appear from the plot that increasing the total water content reduces

the amount of time taken to produce rain. The gure also suggests that there is a minimum water content below which the model does not produce rain, and we can observe that this minimum value is about ($0.1\ gm^{-3}$). It makes sense in practice for such a minimum to exist, because if the total water mass is less than the mass of a 1mm drop, then even if every drop collided and coalesced to eventually form just 1 drop, it would still be too small to be classed as a rain. From the gure it is obvious that in logarithmic axis the

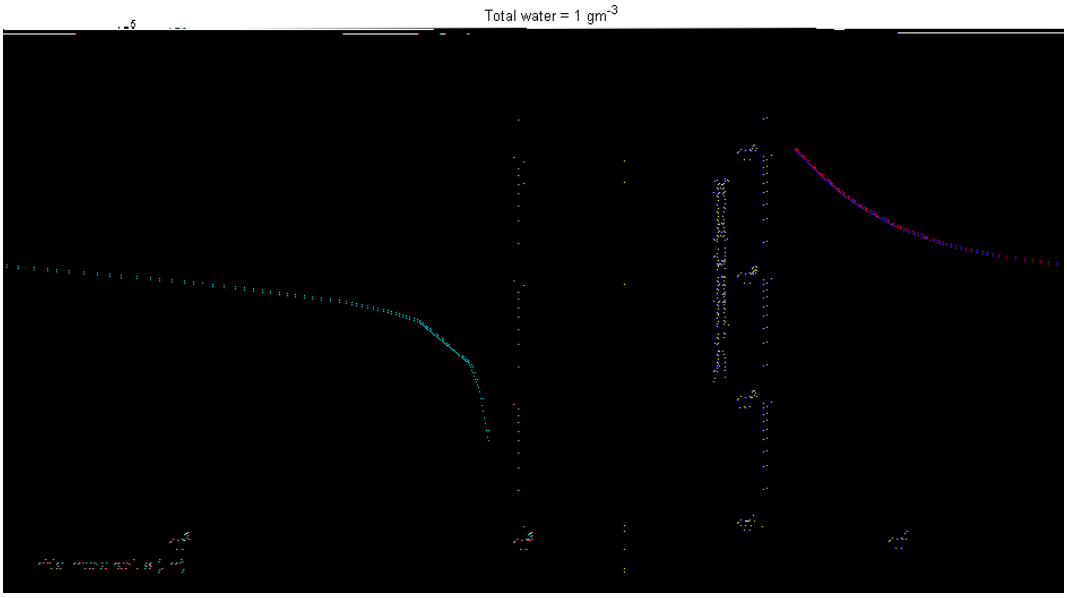

Figure 3.3: Time taken to produce rain for varied initial mode radii but with the total water content xed at 1 gm^{-3}

We now again investigate the time taken for the model to produce rain, but this time through modifying the initial mode radius as shown in gure 3.3. The total water content is kept constant at 1 gm^{-3} in this analysis, so through increasing the initial mode radius we get fewer, but larger drops. Clearly if we decrease this initial radius we will get smaller drops, but of a greater concentration.

First of all from gure 3.3 we can see that for an initial mode radius of 10 m the time taken to produce rain is close to 40 minutes, which is consistent with gure 3.1. If this initial radius is increased the time taken to produce rain can be observed to reduce, and likewise reducing the initial radii

results in an increasingly longer time taken to achieve rain. It seems from the gure that if the mode radius too small, rain is never produced, which we would expect from the previous work in this eld. Figure 3.3 suggests that the initial mode radius must be greater than about 5 m for the collision and coalescence mechanism to produce rain. Through examining the starting distributions for initial mode radii of 4 and 5 m (gure 3.4), we can observe that for the larger of the two sizes, there are substantially more drops close to and above 10 m. The fact that an initial mode radius of 5 m produces rain, but one of 4 m does not, is actually very much in line with the ndings of Davis and Sartor, as they suggested that the collector drops must be larger than 10 m for growth to occur by collision and coalescence.

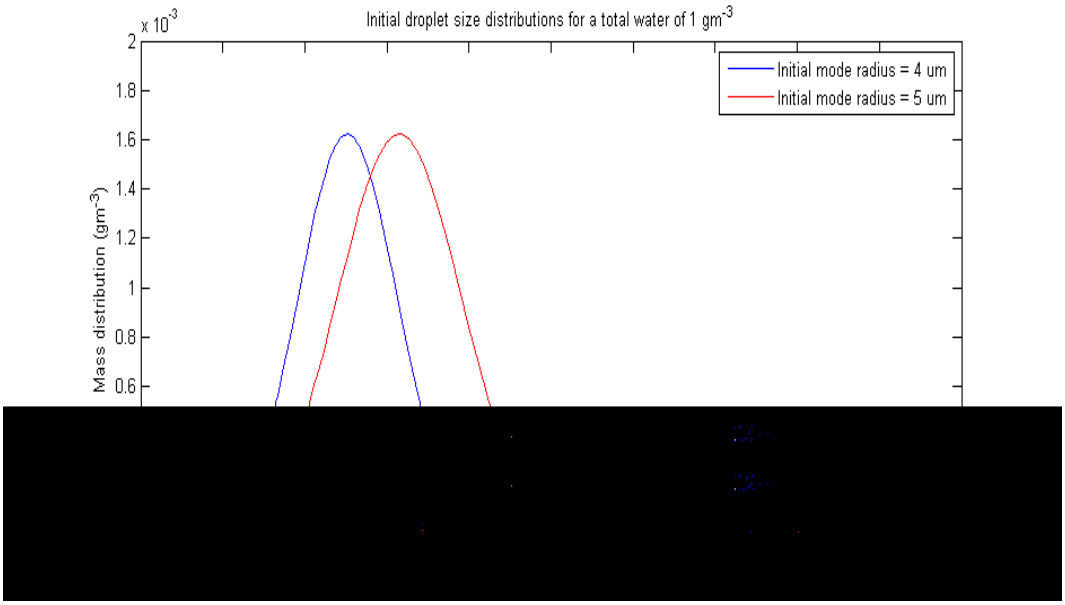

Figure 3.4: Initial droplet size distributions for mode radii of 4 and 5 *m*

Figure 3.3 indicates that the relationship is more complex compared to that between the time to produce rain and the total water content. The rst aspect to note is that there appears a region on the graph between initial mode radii of 20 and 300 m where the gradient is almost constant. The gradient in this region is about -1.1, and so the relation $t / r^{1:1}$ approximately holds between the radii speci ed. To the left of this region, the gradient gradually becomes steeper as the radius decreases, until the minimum initial mode radius required to produce rain is reached. To the right of the straight region, a comparatively rapid steepening of the gradient occurs. It is this region we now investigate to nd a best t to the curve.

From a theoretical perspective if we have initial cloud drops of uniform mass,

then

$$m = \frac{w}{n} \tag{3.1}$$

where w

Here v we may perturb to achieve the best fit, r_1 in the context of the problem we are considering corresponds to the critical radius at which the time taken to produce rain (t) becomes zero (which we can approximately read off figure 3.3 as 0.08 cm), r_0 represents the initial mode radius of the drops, and a we can perturb to make the relationship between t and r either linear, quadratic, cubic or higher order. It should be noted that r_1 may also be perturbed slightly to improve the fit of the curve to the actual solution.

Equation (3.6) suggested that cubic behaviour should give the best fit to the actual data, however this result was derived at constant collision kernel, which we know not be the case in the model, and so we will investigate a range of values for a.

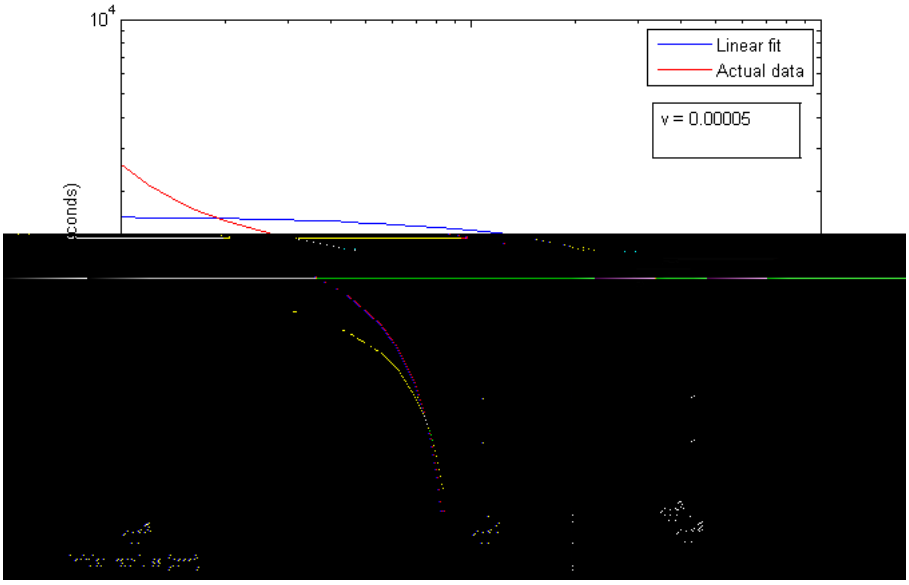

Figure 3.5: Comparing the time taken to produce rain from a tting curve with a=1, v = 0.00005 and r_1 = 0.0800cm to the actual data

If we rst try a linear t (a = 1), we can achieve a solution (gure 3.5) that is somewhat comparable to the actual data with v = 0:00005 and r_1 = 0.0800 cm. The tting curve generally however has too steeper gradient in the region of interest, as the values of the time taken to produce rain go from being overestimates (in the region between r_0 = 0.002 and 0.07 cm) to being underestimates for r_0 > 0:07 cm. From this analysis it would appear that the relationship between t and r is not linear, so we now try greater values of a.

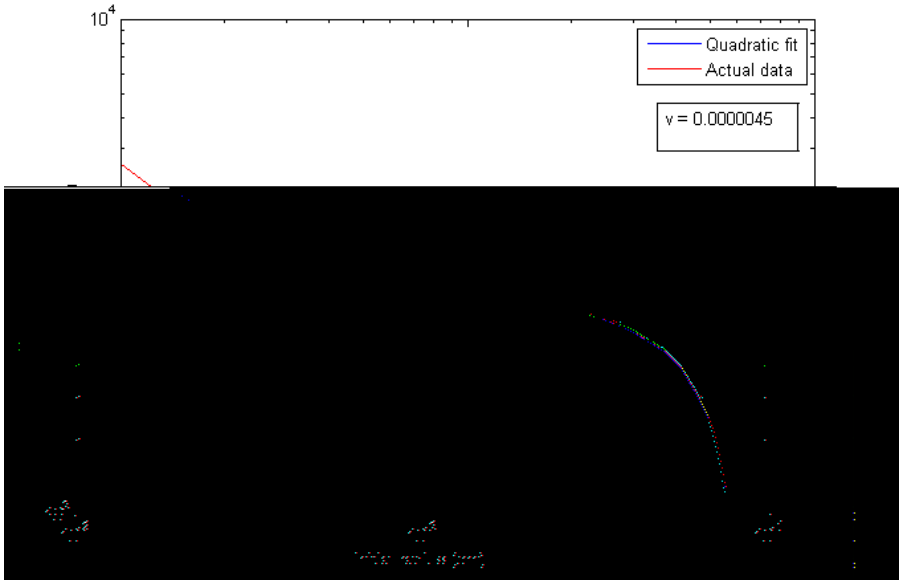

Figure 3.6: Comparing the time taken to produce rain from a tting curve with a=2, v = 0.0000045 and r_1 = 0.0821cm to the actual data

Figure 3.6 illustrates that a quadratic relation (a = 2) with v = 0:0000045 and r_1 = 0.0821 cm gives a very good representation of the actual data in the region we are concentrating on. The rate of negative increase of the gradient is simulated much better than it was with the linear t,tationalsoith thetime to rain values match much better to those of the actual data. If we examine the gure close enough it can be seen however that the rate of change of the

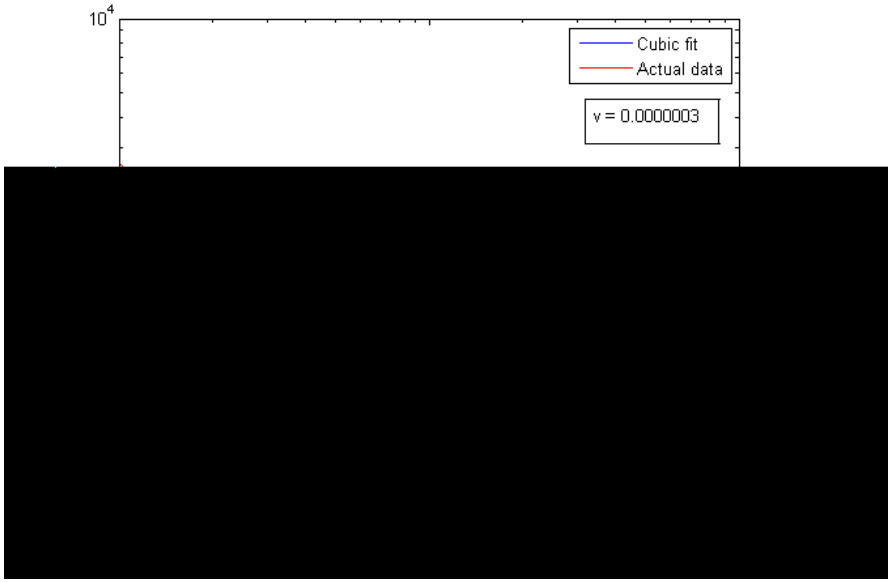

Figure 3.7: Comparing the time taken to produce rain from a tting curve with a=3, v = 0.0000003 and r_1 = 0.0820cm to the actual data

From gure 3.7 we can observe that for v = 0:0000003 and r_1 = 0:0820 cm (which gives the best t for this value of a), the solution is more accurate than the linear one, but less so compared to the quadratic. This analysis is therefore not consistent with equation (3.6) which suggested cubic behaviour should give the best t. The solution is however not substantially less accurate compared to that for a = 2, particularly in the region of r_0 > 0:04 cm. It is clear that the change in gradient appears once again to be somewhat too rapid close to r_1.

The results we have examined suggest that as we increase the value of a, the radius at which the gradient of the solution begins to change is becoming

larger, and certainly it would seem from gure 3.7 that the change in gradient starts at too large a radius. We therefore will not consider larger values of *a*.

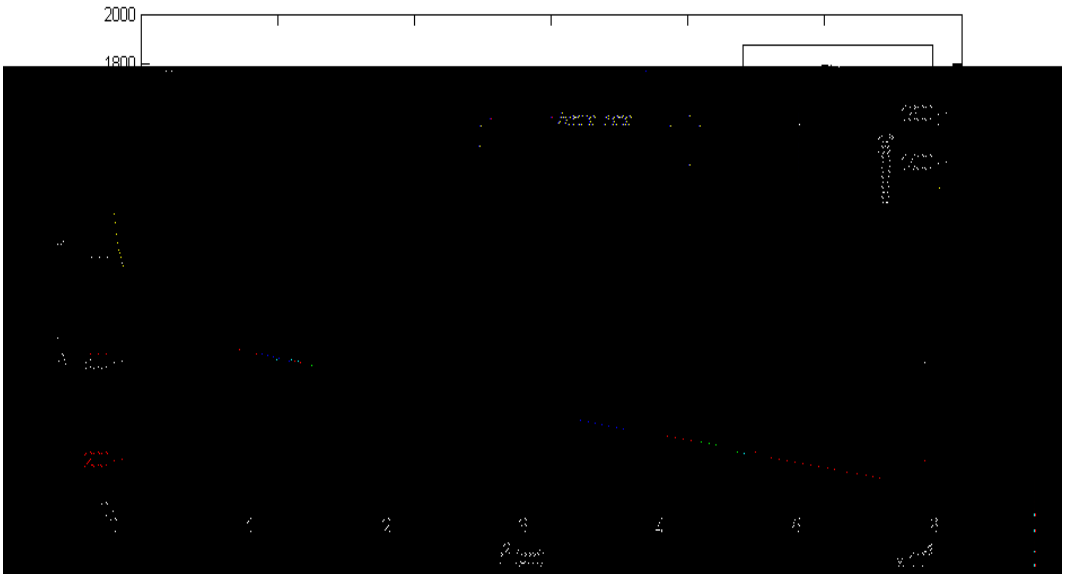

Figure 3.8: Variation of the time taken to produce rain with the square of the initial radius for a=2 as in gure 3.6

We can shown the quality of t more accurately for the quadratic relation ($a = 2$) as illustrated in gure 3.8 by plotting the time to rain against the square of the initial mode radius. From this it is clear that the t is not quite perfect as the gradient of the tting curve is slightly steeper than the curve corresponding to the actual data, which is what we were able to determine from gure 3.6. However the di erences are very minor and to good

We consider the initial distribution shown in gure 3.9 where both peaks are gaussian and identical. The peaks are centred at radii of approximately 5 *m* and 30 *m* respectively. The mass of the drops in the peaks is also shown in the right hand plot, as the results that follow will consider the evolution of the droplet masses rather than radii.

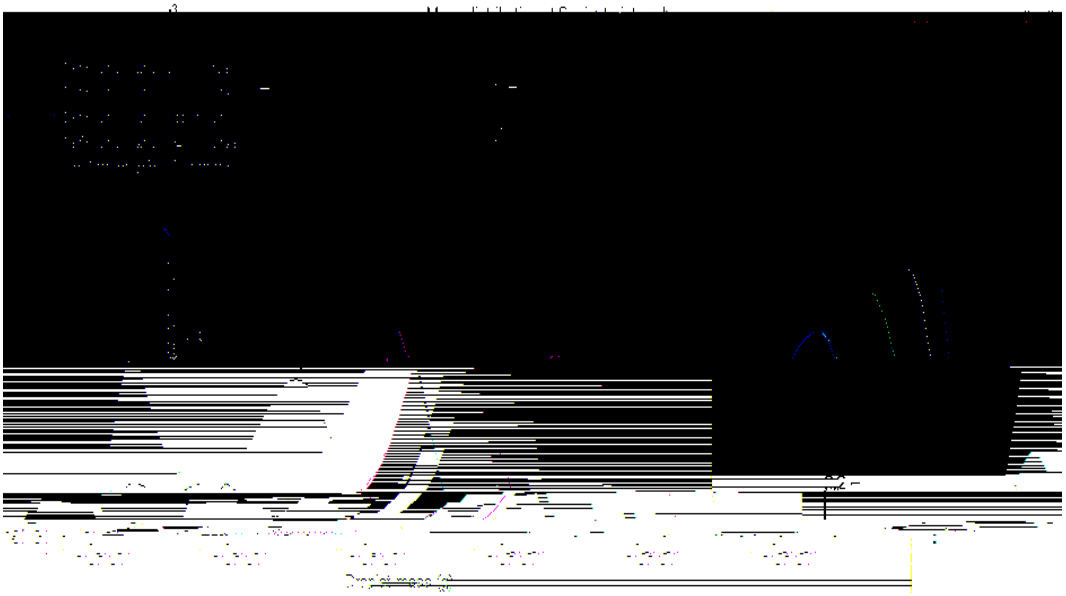

Figure 3.10: Droplet mass evolution from the intial distribution shown in gure 3.9

If we rst just examine the evolution of the droplet masses with time for the initial distribution with two peaks shown in gure 3.9, we observe that after 6 minutes (gure 3.10), both the initial peaks have lost mass (but are still evident), and a third peak has formed centred close to 2 10 ^{3} g. This

third peak can be seen to gain mass at the expense of the initial two for the remainder of the evolution, and also it can be seen to move to the right in the gure (indicating that larger drops are being formed with time).

Theoretically we would expect the droplet number concentrations in the smaller radii peak (n_1) and larger radii peak (n_2) to decrease at the following rates:

$$\frac{dn_1}{dt} = \quad n_1 n_2 \tag{3.9}$$

$$\frac{dn_2}{dt} = \quad n_1 n_2 \tag{3.10}$$

forming new drops of mass $m_3 = m_1 + m_2$ at a rate

$$\frac{dn_3}{dt} = \quad n_1 n_2: \tag{3.11}$$

In 3.9 and 3.10 represents the interaction rate of the droplets (the collision kernel), which as in the previous theoretical derivation is taken to be constant. In this theoretical example we are just considering drops of mass m_1 and m_2, meaning that the initial distribution is in the form of two spikes at these droplet masses rather than a gaussian curve. Also collisions are not considered to occur between drops of the same mass, which is in fact a true statement if we refer back to equation (1.18) since $w(r_i)$ $w(r_j)$ will be zero. Since m_1 is small, m_2 and m_3 are close together, and so we can replace the two spikes at m_2 and m_3 with a single spike of mass:

$$m_l = \frac{n_2 m_2 + n_3 m_3}{n_2 + n_3} \tag{3.12}$$

and drop number concentration,

$$n_l = n_2 + n_3: \tag{3.13}$$

Since n_3 will increase at the expense of n_2, we see that m_l increases at the following rate:

$$m_l = m_2 + \frac{n_3}{n_2 + n_3} m_1; \tag{3.14}$$

so that,

$$\frac{dm_l}{dt} = \frac{dn_3 = dt}{n_2 + n_3} m_1 = \frac{n_1 n_2}{n_2 + n_3} m_1: \tag{3.15}$$

After the first timestep (for which $n_3 = 0$) we associate the new peak at m_l with m_2 (and n_l with n_2) and set $n_3 = 0$ again. We therefore find that:

$$\frac{dn_1}{dt} = n_1 n_2 \tag{3.16}$$

$$\frac{dn_2}{dt} = 0 \tag{3.17}$$

$$\frac{dm_l}{dt} = n_1 m_1 \tag{3.18}$$

We would expect this simplification of the initial distribution (from gaussian

curves to single spikes) in gure 3.9 to give a mass evolution that has reasonable similarity to that shown in gure 3.10. It is however immediately

It is apparent from gure 3.11 that the formation of the larger drops is slightly slower when this di erent collision e ciency is considered (compared to gure 3.10), however the results still disagree with the evolution we would expect from the theoretical approach. To try to explain this we must remember that we have not considered a gaussian distribution in the theory, and so we are missing some larger (and indeed smaller) drops compared to the distribution in gure 3.9. Also the collision kernel is taken to be constant which we know not to be the case from equation (1.18). It seems unlikely that the extra smaller drops are of critical importance (since no combination of them can really produce the mass evolutions shown in gures 3.10 and 3.11). It is however possible that the few very largest drops in the larger radii gaussian peak that are not considered by the theoretical calculations could be of critical importance in explaining the evolutions that the gures show.

So we are proposing that it is the very largest drops that dominate the growth process and that they are necessary for rain to be formed. The problem is however that the number concentration of drops of this size is comparatively very low to those of smaller size, and so it seems that for these drops to be important, they must have a

pute the components that contribute to the kernel, to try to nd the main reason or reasons for the changes in value.

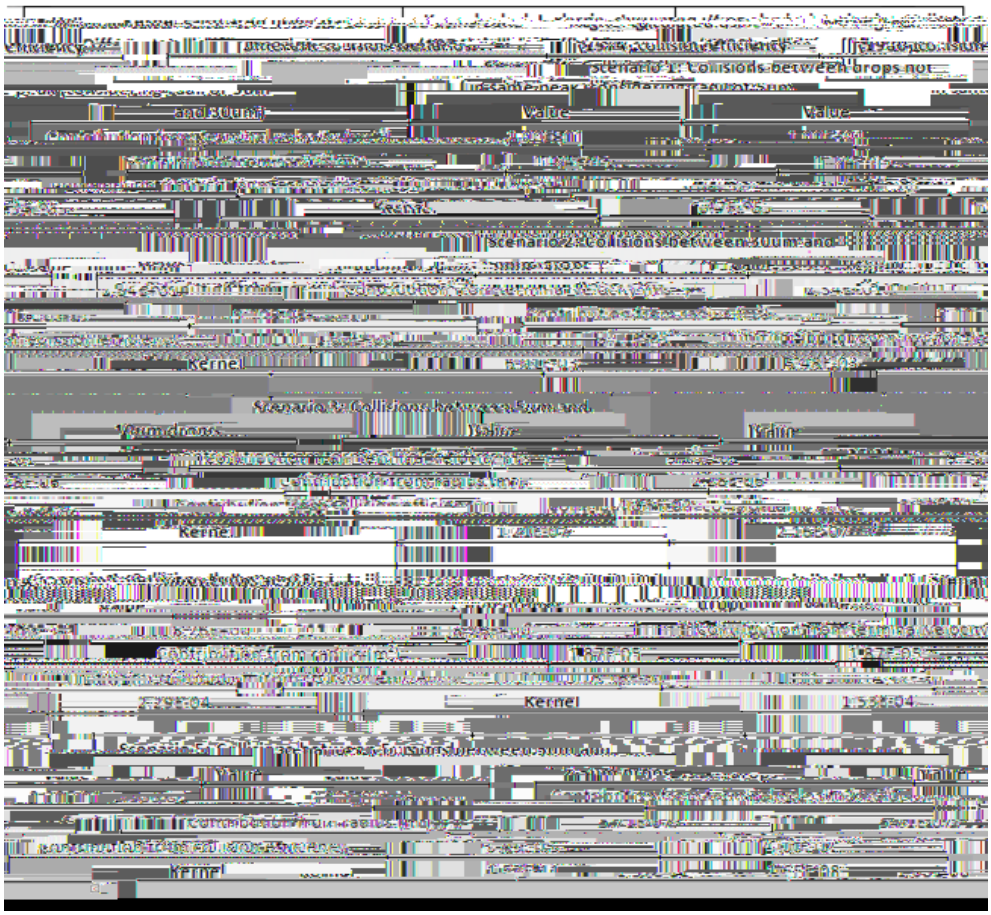

Figure 3.12: Table showing the components of the Kernel with the collision e ciency calculated according to Long (1974) and Hall (1980)

In gure 3.12 we have compared the components that make up the kernel, and the kernel itself for di erent possible colliding scenarios for the initial

two peak distribution we have been considering. If we first just consider the value of the kernel when the collision efficiency from Long is used, we can see that for collisions between drops not in the same peak it has value of order 10^{-5}. This value is a factor of 100 smaller than the kernel for collisions between the very largest drops in the initial distribution (radii of 60 μm) and averaged sized drops in the larger radii peak (30 μm radius). Also if we consider collisions between averaged sized drops in the smaller radii peak (5 μm

used, the dominant component that causes the rapid change in kernel value with drop size is the collision e ciency. It should be noted however that all

We can relate these findings to figures 3.10 and 3.11 to see if we can now better explain the differences in the evolution of the droplet masses. Firstly figure 3.12 showed that the Long efficiency is about 3 times greater than that

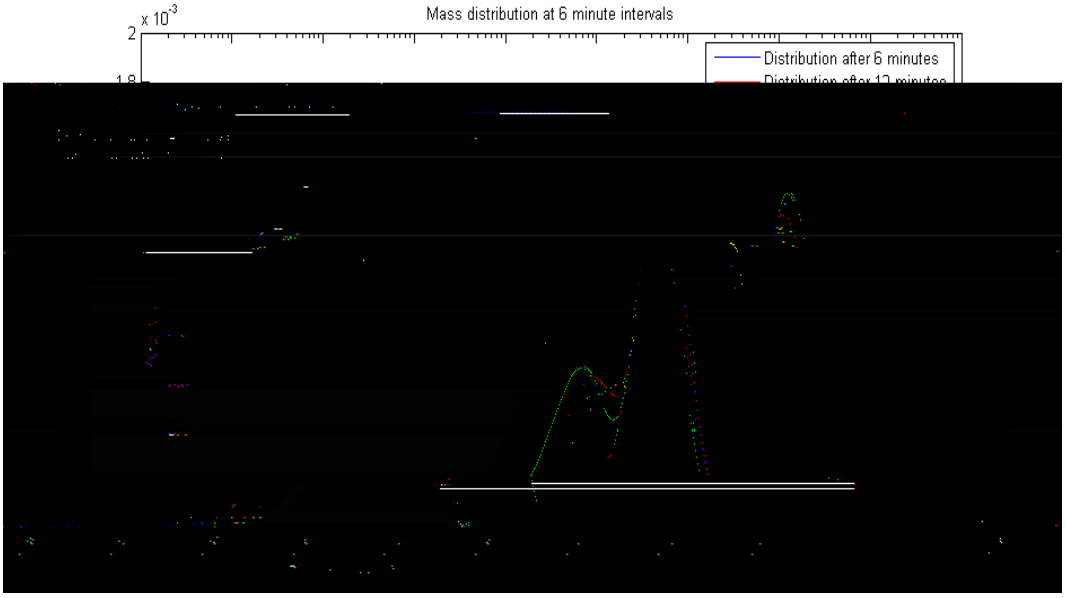

Figure 3.13: Evolution of the droplet masses for a xed collision kernel of 0.00001

The e ect of xing the kernel to 0.00001 is clearly quite profound (gure 3.13) as large drops of rain size do not form, and the larger peak that does form has mass that is simply the progressive sum of the smaller and larger initial drops. From this evidence it is clear that the rapid increase in the kernel with droplet size is of great importance for the formation of rain, as is the presence of a few larger drops (that we have from a gaussian distribution).

Chapter 4

Conclusion

In conclusion we have been able to obtain useful results for the perturbations considered to the initial cloud droplet distribution. Through examining the droplet size evolution with time for the initial conditions considered by Bott, we were able to show that once a few larger droplets have formed, the small initial drops are very rapidly collected by these large drops, and all the water mass in the cloud quickly shifts to be just in large droplets. This could be explained by the theory and equations in the model, which showed that larger drops collide and coalesce with other drops more readily than smaller drops.

We then investigated changing the total water content within the cloud, and were able to show that if we increase the amount of water, the model produces drops of rain size more quickly. It was hence possible to con rm that the relationship t / w^{1} is valid for all water contents. The relationship between the initial mode radius of the cloud drops and the time taken to

produce rain was more complex, although it was obvious that if the initial radius was increased for a xed total water content, drops of rain size were produced more rapidly. For an initial mode radius 20 m r 300 m the relationship $t / r^{1:1}$ approximately holds. For $r > 300$ m we investigated a relationship of the form

$$t = \frac{(r_1^a \quad r_0^a)}{av}$$

and tried to achieve the best t to the actual data with $a = 1;2;3$ corresponding to a linear, quadratic and cubic relationship. The best match was achieved with $a = 2$ (a quadratic t), $v = 0{:}0000045$ and $r_1 = 0.0821$ cm. Therefore for $r > 300$ m it seemed that to good approximation t / r^2. This result disagreed with the cubic behaviour that was expected from a theoretical result derived at constant kernel, with the best explanation for this being that the variation of the kernel with colliding drop radii is very important and cannot be neglected (which we later showed to be the case).

It appeared that to produce rain drops the initial mode radius had to be at least 5 m, and through analysing the initial droplet size distribution that this corresponds to we were able to support the claims of Davis and Sartor that collector drop radii must be at least 10 m for droplets to grow by collision and coalescence. The conclusion here is that drops of radius less than 10 m will not collide and coalesce with similar size drops. The reason for this is that drops of this size have little di erence in terminal velocity. The combination of this and the fact that such drops have little inertia to motion,

means they will follow the air ow around each other rather than colliding.

Through considering an initial droplet distribution with two peaks we were able to show that the model shifts much of the initial mass into substantially larger drops very quickly. This rate of larger drop formation could not be explained by simple theoretical calculations derived at constant kernel, which considered collisions between drops of size equal to the mean size in each peak. This was also true when the collision kernel was adapted in the model to include the collision e ciency from Hall as opposed to that from Long. It seemed likely therefore that not accounting for the few larger drops with higher collision kernel in this initial distribution, was causing the theoretical calculations to disagree. However since the number concentration of such drops was so low, it appeared likely that the chance of these drops colliding and coalescing was not just gradually increasing with colliding drop radii, but actually rapidly increasing.

Through investigating the values of the collision kernel we were able to show

higher, compared to the chance for smaller drops.

It was shown that out of the three components that make up the kernel, the dominant one that causes much of the increase in kernel value with colliding drop radii was the collision e ciency, when it was calculated according

seemingly realistic growth rates from cloud droplet distributions that may or may not be realistic. For this reason it would be ideal to test this model on a known real distribution in a cloud (although it would be di cult to ever

Chapter 5

References

Hocking, L. M., 1959: The collision e ciency of small drops. *Quart. J. Roy. Meteor. Soc.,* 85, 44-50.

Davis, M. H., and J.D. Sartor, 1967: Theoretical collision e ciencies for small cloud droplets in Stokes ow. *Nature.,* 215, 1371-1372.

and coalescence parameters for droplet pairs with radii up to 300 microns. *J. Atmos. Sci.,* 28, 741-751.

Klett, J. D., and M. H. Davis, 1973: Theoretical collision e ciencies of cloud droplets at small Reynods numbers. *J. Atmos. Sci.,* 30, 107-117.

Beard, K. V., and H.T. Ochs, 1984: Collection and coalescence e ciencies for accretion. *J. Geophs. Res.,* 89, 7165-7169.

Long, A., 1974: Solutions to the droplet collection equation for polynomial kernels. *J. Atmos. Sci.,* **31**, 1040-1052.

Hall, W. D., 1980: A detailed microphysical model within two-dimensional dynamic framework: Model description and preliminary results. *J. Atmos. Sci.,* **37**, 2486-2507.